Journal of Coastal Research	33	6	1423–1435	Coconut Creek, Florida	November 2017

A Study of Storm Surge Disasters Based on Extreme Value Distribution Theory

Shuo Yang[†], Xin Liu[‡], Qiang Liu[†]*, Li Guan[†], Jae Myung Lee[§], and Kwang Hyo Jung[§]

[†]Engineering College
Ocean University of China
Qingdao 266100, China

[‡]Australian Joint Research Centre for Building Information Modelling
School of Built Environment
Curtin University
Bentley, WA 6102, Australia

[§]Department of Naval Architecture and Ocean Engineering
Pusan National University
Busan 609-735, Republic of Korea

www.cerf-jcr.org

www.JCRonline.org

ABSTRACT

Yang, S.; Liu, X.; Liu, Q.; Guan, L.; Lee, J.M., and Jung, K.H., 2017. A study of storm surge disasters based on extreme value distribution theory. *Journal of Coastal Research,* 33(6), 1423–1435. Coconut Creek (Florida), ISSN 0749-0208.

In this study, a statistical model was set up using extreme value distribution theory to estimate the return periods for both the highest surge levels and the adjusted direct economic losses from storm surge disasters based on the historical database. The extreme value distribution theory has been widely applied in hydrology and coastal engineering, and one well-performing extreme distribution is the Gumbel distribution. Based on the Gumbel distribution, three parameter estimation methods were used to determine the best method for generating the Gumbel distribution functions; subsequently, the expressions for the return periods were derived. The least square method was identified as the best parameter-estimation method for this study. Comparisons were implemented among return periods of the highest surge levels with the adjusted direct economic loss, which showed that the linear functional relationship between these two indicators was not significant. This study also found there was strong spatial autocorrelation for the highest surge levels with the adjusted direct economic loss by employing spatial analysis along the China's coastline. Analysis based on comparisons among the return periods of the highest surge levels and the adjusted direct economic loss in three coastal regions showed different levels of return periods the regions tended to have. Furthermore, analysis of the variation in indicators between the former half and the latter half of the study period reflected the change in climate. The application of the extreme value distribution theory was extended to evaluate economic losses during a storm surge disaster, and the underlying relationships and the deviations between the highest surge levels and the adjusted direct economic loss were analyzed, which indicated the damages caused by storm surges did not completely depend on the surge level.

ADDITIONAL INDEX WORDS: *Gumbel distribution, return period, highest surge level, economic loss, risk assessment.*

INTRODUCTION

In the past few years, coastal hazards have drawn large attention around the world, whereas storm surge has emerged as one of the most devastating hazards that occasionally cause huge losses in terms of lives and properties (Horn, 2015). Because of the recent trend of global climate change and sea-level variation (Nicholls and Cazenave, 2010) associated with the rapid economic development of coastal areas, the disaster risks caused by storm surges may become increasingly severe. Although there is no evident tendency in the past two decades (Shi *et al.*, 2015), the average annual direct economic losses reached 1.7 billion USD in China in the past 14 years (State Oceanic Administration, P.R.C., 2015). In China, storm surge has been listed as one of the major disasters in the past decades. For example, in 2014 and 2015, the proportions of direct economic losses from storm surge were 99.7% and 99.8%, respectively, out of all the main marine and coastal disasters (State Oceanic Administration, P.R.C., 2015).

The significance of studying storm surge in China arises also because of the upward trend in storm-surge disasters that has occurred along the China coastline. For example, Shi *et al.* (2015) drew a conclusion, based on statistics of extratropical storm surges and typhoon storm surges, that the frequency of storm-surge events in China has increased remarkably since 1949; after statistical analyses of the storm surges since the 1950s in China, Fan (2006) concluded that there was a general increasing tendency for disastrous storm surges.

In hydrology and coastal engineering, the return periods of certain water-level indicators and their corresponding, derived frequencies are viewed as effective and have been widely used to assess the potential risk. Previous studies of the return period based on extreme value distribution theory have achieved valuable results (Coles, 2001). The most common distribution functions include the applied Gumbel distribution, Pearson-III distribution, and the generalized extreme value (GEV) (Obeysekera and Park, 2013; Zhou *et al.*, 2014). For example, statistical frequency analysis using extreme value distribution has been widely used in hydrology to estimate the relationship between the magnitude and the occurrence frequency of various hydrological events (Mahdi and Ashkar, 2004). In addition, Pearson-III distribution, Gumbel distribution, Weibull distribution, and logarithmic normal distribution have been widely used in hydrological statistical analyses (Nnaji *et al.*, 2014).

The calculation of the return period for maximum surge heights at a coastal hydrological station is essential for coastal disaster prediction, coastal engineering design, and estimating the damage of the disaster caused by a storm surge (Kim, Choi,

DOI: 10.2112/JCOASTRES-D-16-00041.1 received 12 March 2016; accepted in revision 6 January 2017; corrected proofs received 12 March 2017; published pre-print online 7 July 2017.
*Corresponding author: liuqiang@ouc.edu.cn

and Cho, 2012; Tsai *et al.*, 2006). Wang and Chen (1984) applied the Gumbel method and an equivalent Pearson-III method to calculate the return period of the surge height at 17 coastal stations. Hu *et al.* (1993) then generalized the Gumbel extreme distribution method for several types of climate extremes, such as the annual maximum temperature, wind speed, precipitation, and wave height. In their study, the moment method, the Thomas plot method, and the least-square method for estimating the parameters were introduced, and the results indicated that the Thomas plot method had greater accuracy. Zhou *et al.* (2014) conducted frequency analyses to predict extreme precipitation in the Taihu Basin in China using two distribution methods, *i.e.* Pearson-III and GEV, while applying the two parameter-estimation methods (maximum-likelihood estimates and L-moments) to estimate each of the distribution methods. To identify the best-fitting model, χ^2 and Kolmogorov–Smirnov (K–S) tests were performed. Based on the results of those two tests, the GEV distribution model using the L-moment estimation method was evaluated as the best-fitting model to identify and predict precipitation in the Taihu Basin. Feng and Jiang (2015) analyzed extreme water levels at three stations on the northwestern Pacific Rim. They evaluated the performance of four types of extreme distributions, *i.e.* Gumbel, Weibull, GEV, and generalized Pareto (GPD) distributions using maximum-likelihood estimates. Results indicated that the GEV distribution performed best at two of the stations, whereas the Gumbel distribution was the best at the other station.

The probability distribution of extreme values approaches an extreme value distribution when the sample size increases infinitely. The extreme value distributions differ from one another because of the different statistical characteristics of the samples. As long as there is a group of samples that has certain statistical characteristics and a large capacity, extreme value distribution can be established. Similar to the extreme value distribution applied to hydrological statistical analyses, extreme value distribution can also be used to analyze the highest surge levels in coastal areas. As an extension of the classic application of extreme value distribution, statistical data of the direct economic loss with large sample capacity can be estimated by extreme value distribution theory.

Because of the broad influences caused by storm surges (NOAA, 2016), the economic loss cannot be constrained within the range of a station or even a province. However, most previous studies usually focus on a single or several specific stations when applying extreme value distributions to analyze the return periods of storm surges. Although this is adequately accurate for calculating the storm surge return period for local coastlines, it is still not precise enough for risk management of storm surge disasters on a larger scale. In addition, because the availability of the historical storm surge event data is limited, it is more feasible to apply the sampling method to research on extreme storm surge value distributions on a large spatial scale. Therefore, the study area discussed in this article covered the entire area of China. In addition, to explore the geographical features of storm surge events in China, spatial analysis was implemented along the China's coastline.

The moment method, the Thomas plot method, and the least-squares method were chosen to estimate the parameters in the distribution functions in this article. Three probability distribution, parameter-evaluating indicators were chosen, namely, standard deviation, relative error, and the largest K–S statistic.

There is no unified functional relationship between the highest surge level and the direct economic loss in storm surge events. The real situation is much more complex, and the connection may not be linear. However, it is apparent that higher surge levels tend to lead to larger inundation areas and more damaged properties at certain locations at certain times. Analyses were conducted to obtain information on such undetermined relationships, and their deviations were analyzed in this study.

In the following sections, the data sources are presented, and then, the extreme value distribution applied in this study and the three parameter estimation methods are briefly introduced. To analyze the relative errors of these three estimation methods, error evaluation methods are presented. The outcomes of these three parameter estimation methods of the highest surge levels and the adjusted direct economic loss are presented, and the distribution functions of each of them were determined. Based on error-evaluation methods, the best-fit distribution functions are chosen, and the return period expression was identified. Then, the correlation between the return periods of the highest surge levels and the adjusted direct economic loss is analyzed. In addition, geographical features of the highest surge levels and the adjusted direct economic loss along China's coastline were analyzed. At last, based on the results of this study, analysis relating to climate change was conducted.

METHODS

There were three main goals in this study: (1) to determine a well-performing extreme-value distribution for the storm surge level based on historical storm surge level data, which was chosen from the results of three parameter estimation methods that were analyzed by the evaluating indicators; (2) to obtain a well-performing extreme value distribution for the direct economic loss, and then, to use the same methods used for the surge level to estimate the parameter and perform evaluation analyses; and (3) to compare and analyze the *N*-year, return-period results from the probability-distribution function for both the surge level and the direct economic loss. The main research route was organized as shown in Figure 1.

Data Sources

The research area discussed in this article covered the entire coastal area of China, as shown in Figure 2. The data needed for this study were the historical records of storm-surge events in China: the highest surge levels and the direct economic losses. Most of the data were collected from publications of the China Oceanic Disasters Communiqué, edited by the State Oceanic Administration, P.R.C. (2015), whereas other data were cited in research articles that involved storm surge data collection; 88 records of severe storm-surge events during the period between 1989 and 2014 were available for this study. All records covered the most-destructive storm-surge events in those years. This means that there were 88 groups of the highest surge levels and direct economic losses in the 26-year study period. All years of the 26-year study period had at least two records, except for 2004, which had only a single record.

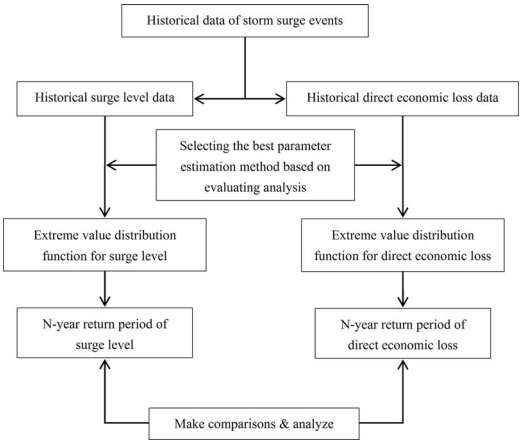

Figure 1. The main research route followed throughout this article.

The most records were from 2005 and 2007, when both years had eight records of severe storm surges.

The records collected were from the most severe storm-surge events in each year, which means that the highest surge levels and/or direct economic losses were the extreme ones in each year. Based on the extreme value distribution theory, only extreme values need to be involved in the calculation of the distribution-function determination process (Gumbel, 1958); as a result, among the 88 records in this study, only the most-extreme records of each year (26 records in 26 years) were included in the calculations. Thus, although the capacity of the database was not abundant, it was sufficient to perform the calculations.

In addition, the economy of China has experienced increasing growth rarely seen in its history. As a result, the value of the loss during storm-surge disasters differed throughout the study period (from 1989 to 2014). Therefore, the gross domestic product (GDP) deflator has been introduced in this article to offset the effects of the rapid economic development experienced in China. The ending year of the research period (2014) was set as the benchmark year for calculating the deflator. Based on data released by the National Bureau of Statistics of the People's Republic of China, *i.e.* the GDP and the GDP index, the GDP deflators for each year during the research period were obtained. All economic data in this article were adjusted by dividing the GDP inflators so that the value of the direct economic loss in each year were comparable according to the price levels in 2014.

Extreme Value Distribution Theory

There are two classes of extreme value distributions in the existing literature (Bali, 2003): (1) the GEV distribution, proposed by Jenkinson (1955), which includes three standard extreme-value distributions, namely Frechet, Weibull, and Gumbel; and (2) the GPD, introduced by Pickands (1975), which has been widely used in financial areas.

The distribution used in this study was based on the classic Gumbel distribution that is a branch of the GEV distribution. The reasons for choosing the Gumbel distribution were based on the following parameters:

- The Gumbel distribution can efficiently use the data and provides acceptable, asymptotic fitting considering the limited data source in this study. (Castillo, 1988; Skjong, Naess, and Naess, 2013; Watt *et al.*, 1989; Yue *et al.*, 1999).
- There are numerous methods for estimating the parameters (Scotto and Tobias, 1999), which confirms its feasibility of the method in this study.
- Because of its wide practical application in hydrology, it is more convenient to compare the research results from this article with those from previous studies. This enables comparable analysis and assists in proving the correctness of the method.

The key features of the GEV distribution are described below. Let $X_1, X_2, \ldots, X_n$ be a sequence of mutually independent, random variables with a common continuous distribution function $G(x)$. Then Y_n is defined as a distribution function equal to $G^n(x)$. Suppose there exists a pair of sequences a_n and b_n, with $a_n > 0$ for all n, and a distribution function $\Lambda(x)$ is defined in Equation (1) (Pickands, 1975):

$$\lim_{n\to\infty} P\left(\frac{Y_n - b_n}{a_n} \le x\right) = \lim_{n\to\infty} G^n(a_n x + b_n) = \Lambda(x) \qquad (1)$$

where, $\Lambda(x)$ is continuous for all x.

The $\Lambda(x)$ is an extreme distribution function that must belong to one of the three generalized extreme distributions (Pickands, 1975). Suppose there are years of data that are recorded daily, for example, the highest surge level, and a sample of the annual maxima is established based on the largest level in each year. The probability of the annual largest values follow the extreme value distribution $\Lambda(x)$ when the sample size is infinite. The choice of the three standard extreme value distributions can be made empirically or be based on a posteriori error analysis.

Gumbel Distribution and Parameter Estimation

The cumulative distribution function (CDF) $F(x)$ of the Gumbel distribution is determined by two parameters, *i.e.* α and β; x is the random variable that stands for the highest surge level or the direct economic loss, in this case. The CDF is shown in Equation (2) (Liu and Ma, 1976):

$$F(x) = \exp\{-\exp[-\alpha(x-\beta)]\} \qquad (2)$$

The values of α and β can be estimated *via* several methods (Scotto and Tobias, 1999; Wang *et al.*, 2012; Zhou *et al.*, 2014). Three methods were used in this study, namely, the moment method, the Thomas plot method, and the least-squares method because they provide good estimation accuracy and calculation convenience for the Gumbel distribution (Öztürk, 2008; Scotto and Tobias, 1999). The accuracy of the different estimation methods may be influenced by the characteristics and size of the sample.

Here, we briefly introduce the three parameter estimation methods. Suppose the ordered sequence from small to large of the historical data is $x_1, x_2, \ldots, x_i, \ldots, x_n$, where x_i is the sequence of the historical data that ranges from small to large, and i is the order of the sequence. $F_n^*(x)$ represents the empirical distribution that can be expressed as Equation (3):

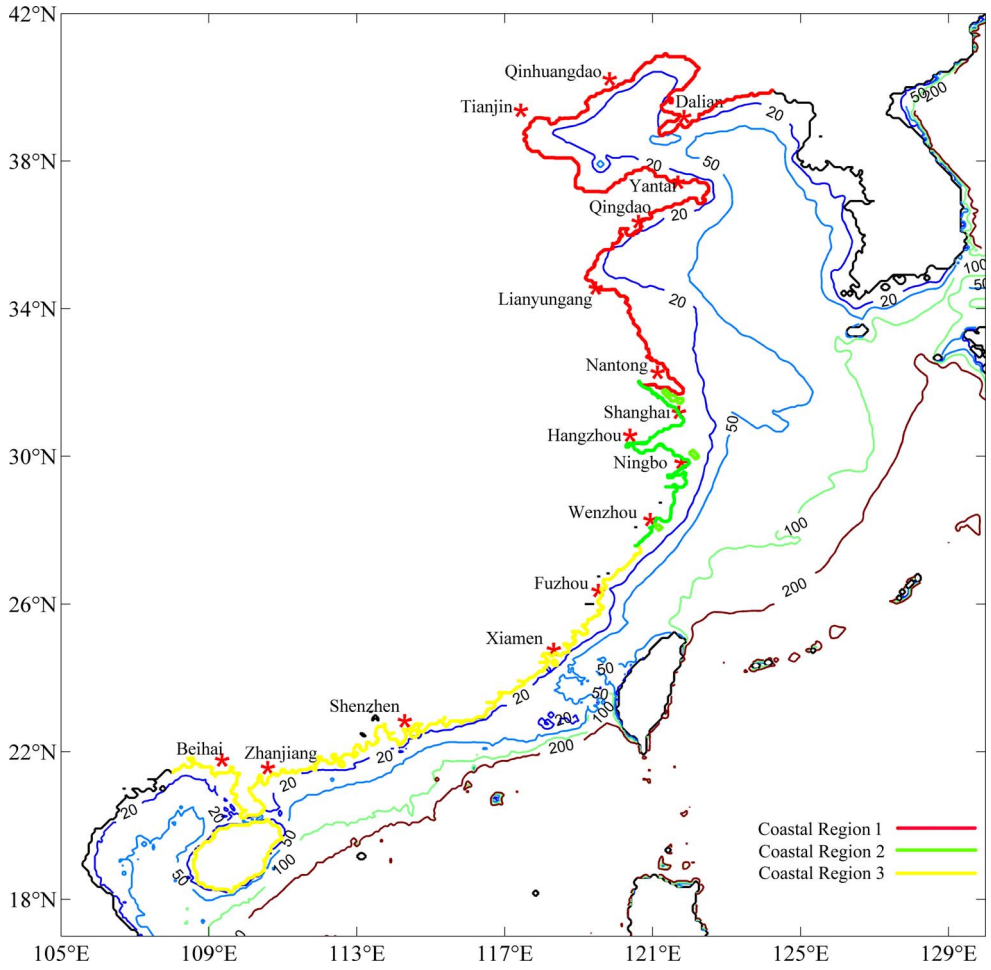

Figure 2. The research area and the major coastal cities listed in the region. (Color for this figure is available in the online version of this paper.)

$$F_n^*(x_i) = \frac{i}{n+1} \qquad (i = 1, 2, \ldots, n) \tag{3}$$

Moment Method

Equation (2) can also be expressed as in Equation (4):

$$F(x) = \exp[-\exp(-y)] \tag{4a}$$

$$y = \alpha(x - \beta) \tag{4b}$$

Equation (4b) can be transformed into Equation (5):

$$\frac{y - \mu_y}{\sigma_y} = \frac{x - \mu_x}{\sigma_x}, \tag{5}$$

where, μ_x and μ_y are the population means of X and Y, and σ_x and σ_y are the standard deviations of X and Y. The values of μ_y and σ_y can be generated based on the moment method:

$$\mu_y = 0.57722 \quad \text{(Euler's constant)} \tag{6a}$$

$$\sigma_y = \frac{\pi}{\sqrt{6}} = 1.28255 \tag{6b}$$

Equation (5) can be transformed into Equation (7):

$$y = \frac{\sigma_y}{\sigma_x}(x - \mu_x) + \mu_y = \frac{\sigma_y}{\sigma_x}\left[x - \left(\mu_x - \frac{\sigma_x}{\sigma_y}\mu_y\right)\right] \tag{7}$$

Compared with Equation (4b), the expressions of α and β can be derived as follows:

$$\alpha = \frac{\sigma_y}{\sigma_x} = \frac{1.28255}{\sigma_x} \tag{8a}$$

$$\beta = \mu_x - \frac{\sigma_x}{\sigma_y}\mu_y = \mu_x - 0.450\sigma_x \tag{8b}$$

$$F(x) = 1 - \frac{1}{T(x)} \tag{9}$$

From Equations (2) and (9), the value of x at the return period of T can be derived as follows:

$$x_T = \beta - \frac{1}{\alpha}\ln\left\{-\ln\left[1 - \frac{1}{T(x)}\right]\right\} \tag{10}$$

The moment method approximates the sample mean $\bar{x}$ and the sample standard deviation S_x, such that they substitute for the population mean and standard deviation. As a result, the CDF and the value of x at the return period are determined by the moment method.

Thomas Plot Method

The moment method makes the sample statistics of x substitute for the population statistics of x. Similarly, the sample statistics of y can also substitute for the population statistics of y. The value of the CDF is assigned, as shown in Equation (11):

$$F^*(x) = \exp[-\exp(-y_i)] = \frac{i}{N+1} \tag{11}$$

$$y_i = -\ln\left[-\ln\left(\frac{i}{N+1}\right)\right] \tag{12}$$

where, N is the sample capacity. Based on the law of large numbers (Hsu and Robbins, 1985), when $N \to \infty$, $F^*(x) \to F(x)$.

The values of μ_y and σ_y are substituted by the sample mean $\bar{y}$ and the sample standard deviation S_y. Then, the expression of CDF can be derived from the combination of Equations (2) and (8), and the expression of x_T is given by Equation (13):

$$x_T = \bar{x} - \frac{S_x}{S_y}\bar{y} - \frac{S_x}{S_y}\ln\left\{-\ln\left[1 - \frac{1}{T(x)}\right]\right\} \tag{13}$$

Least-Squares Method

The least-squares method for mathematical analysis has been widely used in numerous research fields in the past decades. It has been effectively used in the parameter-estimation process in the extreme value distribution. According to Equation (4b), the linear relationship between x and y can be expressed as shown in Equation (14):

$$x = \frac{1}{\alpha}y + \beta \tag{14}$$

Based on the principle of the least-squares method, the coefficient of Equation (14) can be derived as in Equation (15), where r_{xy} is the correlation coefficient between x and y:

$$\frac{1}{\alpha} = r_{xy}\frac{S_x}{S_y} \tag{15a}$$

$$\beta = \bar{x} - \frac{1}{\alpha}\bar{y}, \tag{15b}$$

where, the determination of $\bar{y}$ and S_y are similar to the method used in the Thomas plot. Thus, the CDF and x_T can be derived from Equations (2) and (10).

Error Evaluation Methods

To determine the best parameter-estimation method, the three methods applied were tested by three goodness-of-fit tests: standard deviation σ (Equation 16), relative error V (Equation 17), and the largest K–S statistic D_n (Equation 18):

$$\sigma = \sqrt{\frac{\sum_{i=1}^{n}(x_i - \hat{x}_i)^2}{n-1}} \tag{16}$$

$$V = \frac{1}{n}\sum_{i=1}^{n}\left|\frac{x_i - \hat{x}_i}{\hat{x}_i}\right| \tag{17}$$

$$D_n = \max\left[\left|F_n^*(x) - F(x)\right|\right] \tag{18}$$

Based on the empirical distribution $F_n^*(x)$, the fitted data $\hat{x}_i$ can be derived. Based on the K–S test theory, according to the acceptable level of significance α_s ($\alpha_s = 0.05$ in this case) and the number of data series n, $\hat{D}_n$ can be obtained. If $D_n < \hat{D}_n$, the chosen probability distribution identified fits the observed data series (Zhou *et al.*, 2014).

After the method with the best performance in the goodness-of-fit tests was chosen, the parameters determined from the tests can be substituted into the CDF $F(x)$. As illustrated in Figure 1, this main research route was applied to the calculations for both the highest surge level and the adjusted direct economic loss.

The return period $T(x)$ can be derived from $F(x)$:

$$T(x) = \frac{1}{1 - F(x)} \tag{19}$$

Then, the value of x (the highest surge level or the adjusted direct economic loss) corresponding to its return period can be determined by Equation (10). Through the use of the CDFs (from which the probability distribution functions [PDFs] can be conveniently derived) of the highest surge level and the adjusted direct economic loss, which were determined by different parameter-estimation methods, the return period can be determined for further comparison and analysis.

Furthermore, because both the adjusted direct economic loss and the highest surge level increase have geographic features, their spatial distribution should follow the first law of geography (Tobler, 1970). Therefore, all 88 historical events were geocoded as points on the map, and the classic spatial-analysis method Kriging (Liu *et al.*, 2014; Oliver and Richard, 1990) was applied to them to interpolate their spatial distribution along China's coastline. The spatial coordinates of the georeferenced points indicates where the storm surge events happened historically. The adjusted direct economic loss and the highest surge level are two attributes of the spatial points.

RESULTS

Calculation of the distributions derived from the parameter estimation was performed. The three parameter estimation methods were applied to the distribution analyses of the highest surge levels and the adjusted direct economic loss. The CDFs were determined based on the approaches mentioned above, and the PDFs could be conveniently generated from the CDFs. The relationships between the return period and the highest surge levels or the adjusted direct economic loss were determined. The values corresponding to the typical return periods, which are frequently used in coastal and ocean engineering applications (CCCC First Harbor Consultants Staff, 1998; Dong *et al.*, 2013), are listed separately.

Extreme Distribution Function for Surge Level

The CDFs and PDFs of the three parameter estimation methods were calculated as shown in Figure 3. The values of α

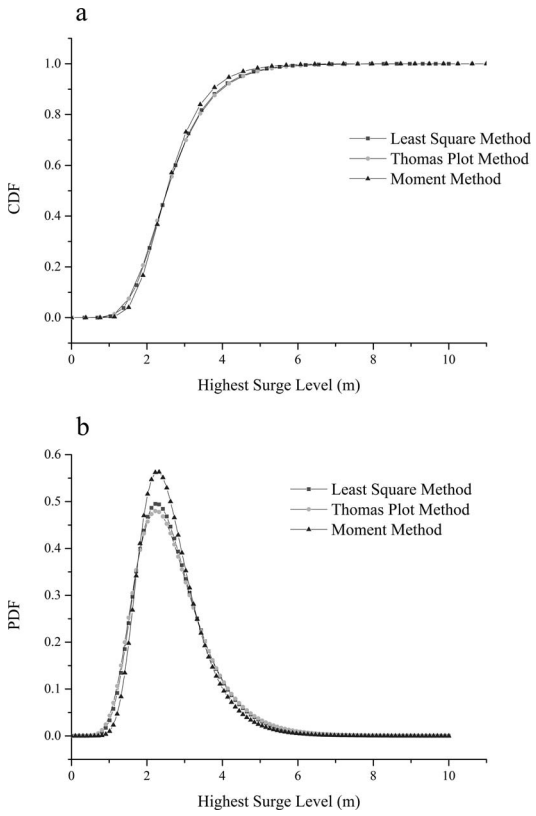

Figure 3. Cumulative distribution functions and probability distribution functions of the highest surge levels from the three parameter estimation methods. (a) CDFs of the highest surge level: the differences between the CDFs are marginal, and the increasing rate of the moment method between the highest surge levels of 1.5 m and 4.5 m is steeper than those of the other methods. (b) PDFs of the highest surge level: the peak value of the moment method is the highest compared with those of the other methods and that of the least-squares method is second and slightly higher than that of the Thomas plot method.

and β in the calculated CDFs are shown in Table 1. Figure 3a shows that the differences between the CDFs were marginal. The increasing rate of the moment method between the highest surge levels of 1.5 m and 4.5 m was steeper than those of the other methods. From Figure 3b, the peak values of the PDFs were different; the peak value of the moment method was the highest compared with those from the other methods, with the least-squares method second and slightly higher than that of the Thomas plot method. However, the values of the PDFs were very similar at the highest surge levels below 1 m and above 6 m.

The relationships between the return period and the highest surge levels were calculated with Equation (19) and are illustrated in Figure 4. The data observed are also presented in Figure 4 for better understanding. Because the return periods in the observable data were relatively short, the expected return periods longer than 30 years cannot be confirmed. In addition, the observable data all fell near the return period lines. The values corresponding to the typical return periods are listed in Table 2.

Table 1. *The values of* α *and* β *in the highest surge-level parameter estimation.*

Parameter Estimation Method	α	β
Least-squares method	1.347	2.260
Thomas plot method	1.305	2.247
Moment method	1.534	2.277

Extreme Distribution Function for Adjusted Direct Economic Loss

The CDFs and PDFs of the three parameter estimation methods were calculated as shown in Figure 5. The values of α and β in the calculated CDFs are shown in Table 3.

As shown in Figure 5a, the differences between the three CDF lines of the adjusted direct economic loss were barely noticeable, except that the line for the moment method rose slightly steeper when the adjusted direct economic loss was less than 3 billion USD. The PDFs are shown in Figure 5b, where the peak values of the three lines were marginally different, with the moment method having the highest peak value, whereas the other two methods had similar lower peak values.

The functional relationships between the return period and the adjusted direct economic loss are illustrated in Figure 6. The observed data for the historical economic loss aligned well with the economic loss lines. The slopes of the least-squares method and the Thomas plot method were similar and steeper, whereas the slope of the moment method was smaller. Most of the observed data fell near the lines, except for two spots whose return periods were more than 10 years and were slightly higher than the lines. The quantity of the observed data was limited. As a result, the functional relationship between the return period and the adjusted direct economic loss can be confirmed merely by the data observed below the return period of approximately 30 years; therefore, the trend in the results beyond that point can only be viewed as theoretical. The values of the typical return period are shown in Table 4.

ANALYSIS

Based on the results calculated in the last section, evaluation of the results was implemented using three goodness-of-fit

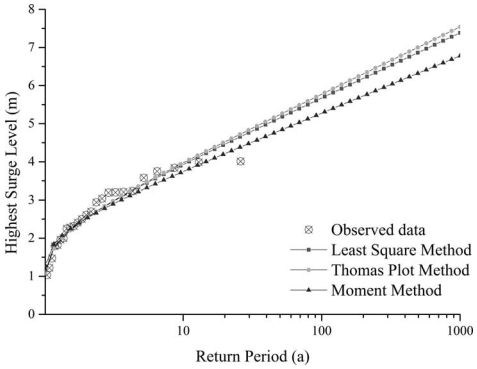

Figure 4. Calculated return periods corresponding to the highest surge levels and the observed data, which illustrate the conformity between the calculated data and the observed data. The observed data all fall near the return period lines.

Table 2. *Predicted* N*-year return-period storm-surge level over one year.*

	Return Periods								
Parameter Estimation Method	1000	500	200	100	50	25	20	10	2
Least-squares method	7.39	6.87	6.19	5.67	5.16	4.63	4.46	3.93	2.53
Thomas plot method	7.51	6.98	6.28	5.74	5.21	4.67	4.49	3.94	2.50
Moment method	6.78	6.33	5.73	5.28	4.82	4.36	4.22	3.75	2.52

parameters, so that the extreme value distributions of the highest surge levels and the adjusted direct economic loss could be determined. Because the return periods of the highest surge level and the adjusted direct economic loss were calculated independently, a comparative analysis was implemented to discuss the inherent relationships between them. Because the calculation of the extreme value distribution was on a national scale, however, the intensity of storm-surge disaster differs geographically; therefore, additional spatial analyses and evaluation in terms of geographical locations were performed. In addition, given the trend of climate change in recent years, storm-surge disaster levels in both halves of the study period (26 y) were calculated, respectively, and compared with each other.

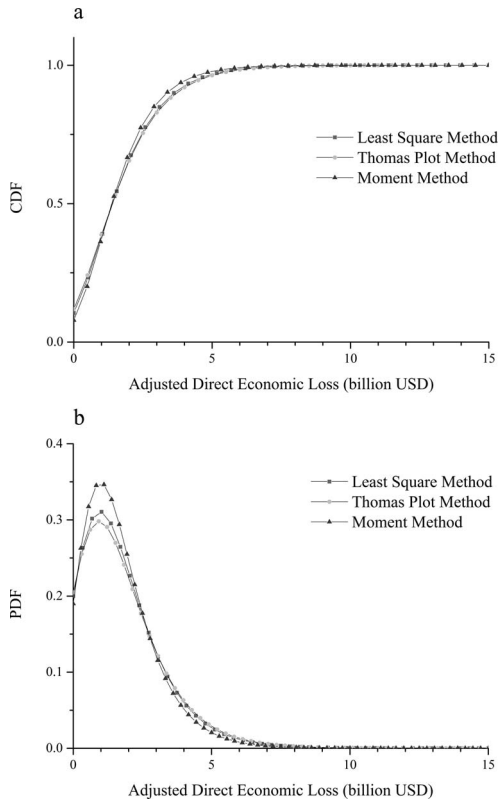

Figure 5. Cumulative distribution functions and probability distribution functions of the adjusted direct economic loss from the three parameter estimation methods. (a) CDFs of the adjusted direct economic loss: the differences among the three CDF lines are barely noticeable. (b) PDFs of the adjusted direct economic loss: the moment method has the highest peak value, whereas the other two methods have similar, lower peak values.

Determination of the Extreme Value Distribution

The expressions of the CDFs, the PDFs, and the return period were determined in the previous section. The distribution functions with the best goodness-of-fit were chosen based on the evaluation results from three goodness-of-fit tests. The goodness-of-fit test results for the highest surge level and the adjusted direct economic loss are listed in Tables 5 and 6, respectively. Given that the acceptable level of significance $\alpha_s = 0.05$ and the number of data series was 26, $\hat{D}_n(0.05) = 0.259$. All values of D_n were smaller than 0.259, which implied that none of the three methods were rejected by the K–S tests for the significance level of 0.05.

For the highest surge level, the least-squares method had the better performance in both goodness-of-fit tests for σ and V. No values for D_n were rejected by the K–S tests (<0.259), whereas the Thomas plot method had a smaller D_n. Therefore, the distribution function estimated by the least-squares method was chosen as the final distribution of the highest surge level for the best goodness-of-fit.

For the adjusted direct economic loss, the σ of the least-squares method had the better performance. None of the values of D_n were rejected by the K–S tests, whereas the moment method had the smallest V out of the three methods. Because the value of V can be influenced by certain fitted data with small absolute values (Equation 17), the value of σ was considered to be the main basis of the evaluation. Therefore, the least-squares method was chosen as the final distribution of the adjusted direct economic loss.

Comparative Analysis

Return periods of the highest surge level and the adjusted direct economic loss were compared and analyzed based on the reported results. After the best parameters for the distribution functions were determined, the N-year return period was generated by the best distribution function with relatively better accuracy. Each storm surge event in the database had a highest storm-surge height and a corresponding adjusted direct economic loss. The return periods of the highest surge level and the adjusted direct economic loss were calculated by choosing the best distribution functions. Therefore, there were two series of return periods generated by the distribution function of the highest surge level and the distribution function of the direct economic loss, respectively. This means that separately calculated return periods for the highest surge level

Table 3. *The values of* α *and* β *in the parameter estimation of the adjusted direct economic loss.*

Parameter Estimation Method	α	β
Least-squares method	0.845	0.962
Thomas plot method	0.810	0.935
Moment method	0.948	0.983

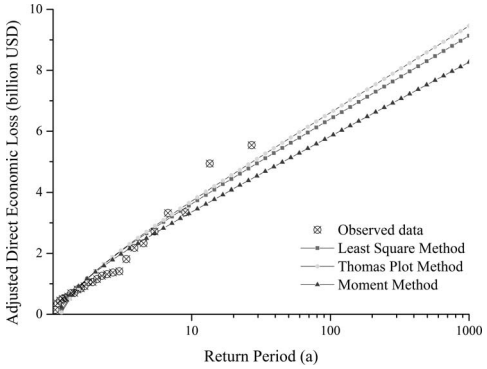

Figure 6. Calculated return periods corresponding to the adjusted direct economic losses and the observed data, which illustrate the conformity between the calculated data and the observed data. Most of the observed data fall near the lines, except for two spots that are slightly higher than the lines.

and the adjusted direct economic loss from the same historical storm-surge event could be different from each other. However, correlations existed between the two series of return periods because of the inherent cause-and-effect relationships. Based on that idea, the comparisons and analyses were implemented.

The 88 historical events were resorted in an ascending order according to the surge level observed, which functioned as a reference. Then, the return periods of the highest surge level and the adjusted direct economic loss were computed separately using the chosen distribution functions. The results are illustrated in Figure 7.

As shown in Figure 7, the movement of the direct economic loss line was not synchronous when the return periods of the highest surge levels increased. The correlation coefficient was 0.02, which represented a linear functional relationship between the two series of return periods, and was not significant. There were more large values from direct economic losses when the return period of the highest surge level increased, whereas not all the events followed that rule. Additionally, the return period of the adjusted direct economic loss tended to be longer than that of the highest surge level when the return period of the highest surge level was shorter than 1.29 years. This was because, out of 50 events, there were only three in which the return periods of the adjusted direct economic loss were shorter than those of the highest surge level, whereas the differences between the return periods of these two indicators of the three events were all less than 0.05 years. In contrast, out of 38 events that had return periods of the highest surge levels that were longer than 1.29 years, there were 27 events that had shorter return periods for the adjusted direct economic loss than they had for the return periods of the corresponding highest surge level. This means that, historically, the storm surge events with minor surge levels have often caused unexpected economic losses.

Table 5. *Goodness-of-fit test results for the Gumbel distribution of the highest surge level.*

Parameter Estimation Method	σ	V	D_n
Least-squares method	0.213	0.061	0.098
Thomas plot method	0.217	0.063	0.093
Moment method	0.237	0.079	0.128

Spatial Analysis

To better investigate the relationship among factors, spatial analysis can be used to evaluate the correlation. Theoretically, nonspatial correlation analysis can lead to biased conclusions. By applying spatial analysis to the adjusted direct economic loss and the highest surge level, this study found there were strong spatial autocorrelation (Figure 8a,b) for both of them. Furthermore, an irrefutable spatial correlation (0.39) was identified between these two factors.

Two high–high areas were found in the south Zhejiang province and at the intersection between Guangdong province and Guangxi province, respectively. Although relatively high surge-level increases were identified in some other areas, such as NE Hainan province and NE Fujian province, the economic losses were relatively small. In contrast, the low levels of the highest surge-level increase did not necessarily mean small economic losses. For example, the area around Shanghai was more sensitive to storm-surge events, and the low level of the highest surge level increase there could lead to moderate economic losses. These findings could have been concealed with nonspatial correlation analysis.

Evaluation Based on Geographic Locations

In this study, the research on extreme value distribution was at a national scale. However, the different economic and topographic characteristics of various geographic locations imply return periods that may differ geographically. To emphasize that consideration, the coastline of China was divided into three parts according to their natural geographic zoning (as shown in Figure 2). The return periods of the highest surge levels and the adjusted direct economic losses in these regions were then analyzed.

The first part (coastal region 1 [CR1]) covered the coastal areas north of the Yangtze River, which included the entire coastline of north China and the northern part of the coastline of the east China. The second part (coastal region 2 [CR2]) included the southern part of the east China region, *i.e.* the coastline of Shanghai City and Zhejiang Province. The third part (coastal region 3 [CR3]) covered the entire coastline of

Table 4. *Predicted* N*-year return-period adjusted direct economic loss over one year.*

	Return Periods								
Parameter Estimation Method	1000	500	200	100	50	25	20	10	2
Least-squares method	9.13	8.31	7.23	6.40	5.58	4.75	4.48	3.62	1.40
Thomas plot method	9.46	8.60	7.47	6.61	5.75	4.88	4.60	3.71	1.39
Moment method	8.27	7.54	6.57	5.83	5.10	4.36	4.11	3.36	1.37

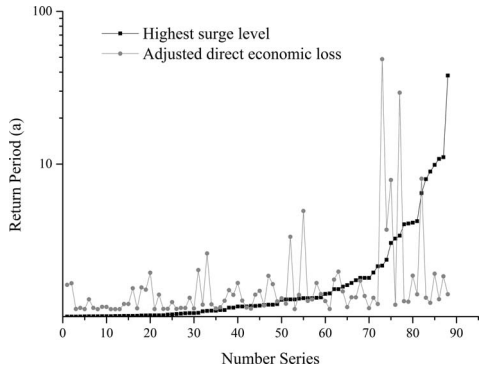

Figure 7. Comparison of the highest surge level with the adjusted direct economic loss, both of which were originated from specific events. As shown, there are some apparent differences between the two lines.

south China. In addition, other types of storm surges besides typhoon storm surges, *i.e.* extratropical storm surges, occur in the coastal areas of the Bohai Sea, the Yellow Sea, and northern part of the east China Sea. The areas influenced by extratropical storm surges overlap the CR1.

In CR1, 11 storm-surge events were recorded during the 26-year research period. The values for those storms are illustrated in Figures 9 and 10. In Figure 9, the observed data from the highest surge level in CR1 were lower than the calculated data. Each value of the highest surge level from the observed data was smaller than that of the calculated value for a similar return period; in other words, the observed data had a parallel trend with the calculated data. The difference in the values between the two groups was stable. The correlation coefficient between the two groups of data was the largest (0.984) among the three regions, which indicated the two

Table 6. *Goodness-of-fit test results for the Gumbel distribution of the adjusted direct economic loss.*

Parameter Estimation Method	σ	V	D_n
Least-squares method	0.392	0.902	0.162
Thomas plot method	0.396	0.924	0.160
Moment method	0.420	0.847	0.153

groups of data of CR1 were the mostly related linearly. The mean value and the standard deviation for the difference in values were 1.736 m and 0.105 m, respectively (see Table 7). The value of the standard deviation was the smallest among the three regions. Although there was insufficient historical data for CR1 to calculate the return-period curve for this region, it still can be concluded that the level of the highest surge level was lower than the level for the country as a whole. The observed data for the adjusted direct economic loss are shown in Figure 10. As shown, the observed values for the adjusted direct economic loss in CR1 were far less than the calculated data at similar return-period levels. The mean difference in the values between the observed data and the calculated data was 2.604 billion USD. The correlation coefficient between the two groups of data was 0.916, and the standard deviation value of the different values was 0.699 billion USD. It can be concluded that, at a similar return-period level, the adjusted direct economic loss in CR1 tends to be less than the adjusted direct economic loss from a national perspective.

In CR2, 16 storm surge events occurred during the 26-year research period. As shown in Figure 9, all the highest surge levels from the observed data were smaller than the values from the calculated data for similar return-period levels. However, the difference in values between the two groups of data was not as large as the differences in CR1 values. The mean difference in values in CR2 was 0.816 m. The correlation

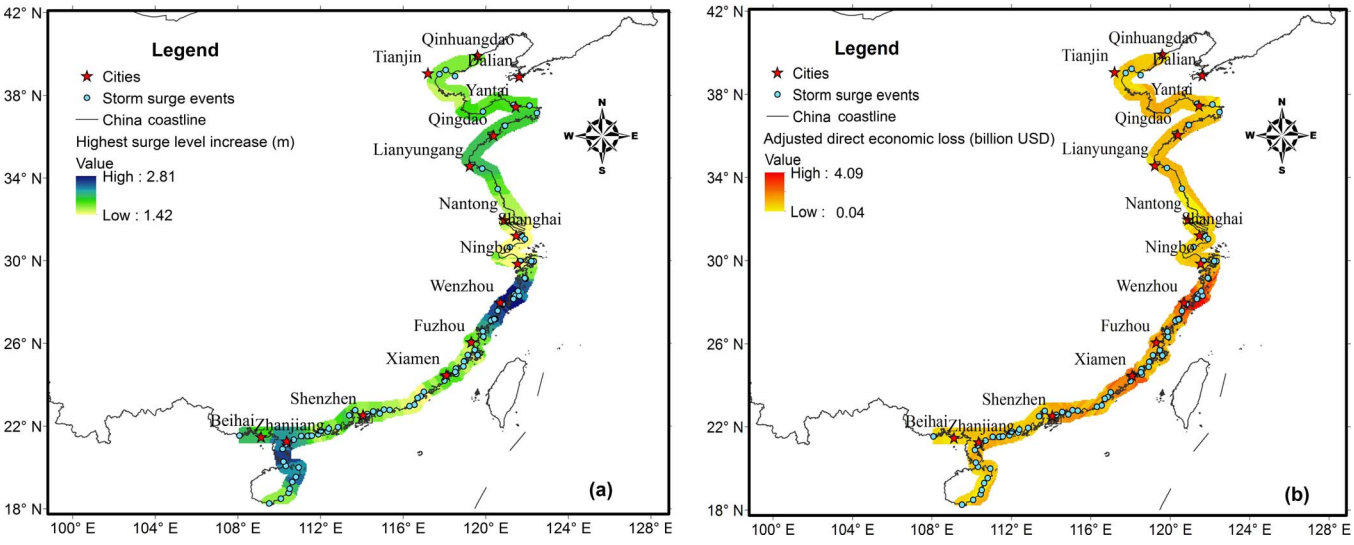

Figure 8. In the coastal section of a map of China, major coastal cities are shown, and the spatial distributions of the highest surge level (a) and the adjusted direct economic loss (b) along the coastline are illustrated. (Color for this figure is available in the online version of this paper.)

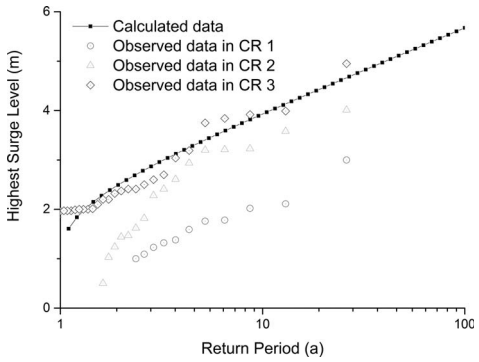

Figure 9. Comparison between the calculated data and the observed data on the highest surge level from the three coastal regions.

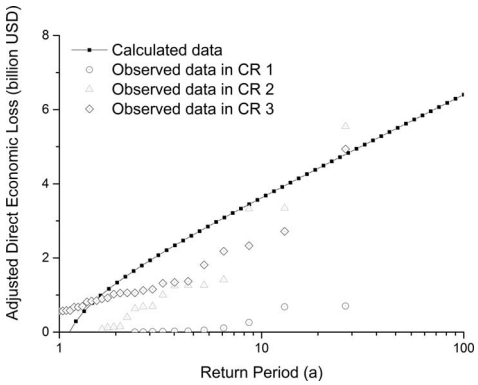

Figure 10. Comparison between the calculated data and the observed data on the adjusted direct economic loss from the three coastal regions.

coefficient between the two groups of data was 0.951. The standard deviation of the difference in values was 0.420 m. The highest surge level in CR2 was still lower than the calculated data but was higher than the observed data in CR1, which indicates the highest surge level in CR2 tended to be higher than that in CR1 and was also closer to the national level. As illustrated in Figure 10, the observed data for the direct economic loss in CR2 were smaller than the calculated data when the return period was less than 20 years. All the observed data in CR2 were higher than the observed data in CR1. The plots of the observed data were close to the calculated line when the return period was larger than 10 years. The mean value of the difference in values between the observed data and the calculated data was 0.975 billion USD. The standard deviation and the correlation coefficient between the two groups of data were 0.560 billion USD and 0.953, respectively. Based on the results shown in Figure 10, storm surges with relatively small economic losses (less than 2 billion USD) happened less frequently in CR2, but storm surges with adjusted direct economic losses greater than 2 billion USD tended to be at similar levels throughout the entire study area.

As illustrated in Figure 9, the observed data of the highest surge level in CR3 were close to the calculated data. The closeness was reflected by the evaluation parameters. The mean value of the difference in values was –0.002. The standard deviation of the mean difference in values was 0.241, and the correlation coefficient between the two groups of data was 0.955. The return period for the highest surge level in CR3 was most similar to the return-period level for the country as a whole, which also means storm surges in CR3 best approximate the extreme level of the highest surges among the three regions of the entire country. As for the adjusted direct economic loss in CR3 (see in Figure 10), the mean difference in the values between the calculated data and the observed data was 0.287 billion USD. The standard deviation of the mean difference in values was 0.624 billion USD, and the correlation coefficient between the two groups of data was 0.893.

Climate Change

The application of the extreme value distribution theory requires a sufficiently long series of historical data. Theoretically, the results will be more accurate with additional historical data for a longer time span, which means studies using extreme value distribution usually use data from years before. To associate those data with the climate-change trends during the past decade, it is necessary to analyze the changes in the indicators during the study period. Comparisons were made between two halves of the study period (13 years each) in terms of the highest surge level and the adjusted direct economic loss.

As shown in Figures 11 and 12, return periods were divided into six groups. The return periods were derived from substitution of the historical storm-surge records into the final distributions that were formerly determined in this study. Because no return period in the historical record exceeded 100 years and all calculated return periods exceeded 1 year, the x-axis started at year 1 and ended at year 100. In Figure 11, the frequency in all return-period groups increased in the second

Table 7. *Evaluation parameters in the three coastal regions of China.*

	Highest Surge Level (m)			Adjusted Direct Economic Loss (billion USD)		
Region	*d*	SD	*r*	*d*	SD	*r*
CR1	1.736	0.105	0.984	2.604	0.699	0.916
CR2	0.816	0.420	0.951	0.975	0.560	0.953
CR3	−0.002	0.241	0.955	0.287	0.624	0.893

CR1 = coastal region 1, covering the coastal areas northern of the Yangtze River, including the entire coastline of the north China and the northern part of the coastline of the east China; CR2 = coastal region 2, covering the southern part of the east China region, i.e. *the coastline of Shanghai City and Zhejiang Province; CR3 = coastal region 3, covering all the entire coastline of the south China;* d = *the mean value of the difference in values between the observed data and the calculated data and equals the calculated data minus the observed data; SD = the standard deviation of the difference in values between the observed data and the calculated data;* r = *the correlation coefficient between the observed data and the calculated data.*

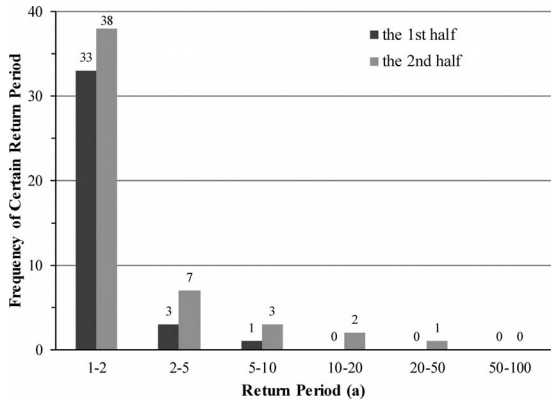

Figure 11. Frequency of certain return periods of the highest surge level, with the research period divided into two halves.

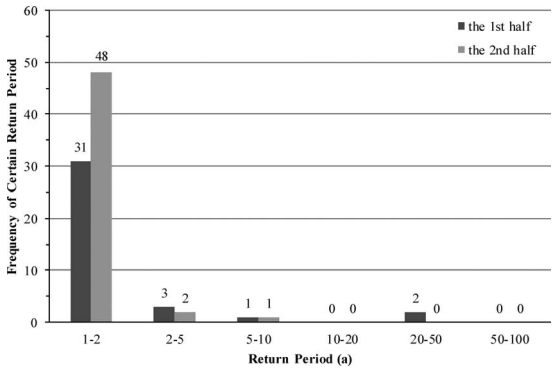

Figure 12. Frequency of certain return period of the adjusted direct economic loss, with the research period divided into two halves.

half, except the last group (50–100 years). The frequency of storm surges with the return period of the highest surge levels from 2–5 years doubled in the second half of the study period, and the return period times in the group of 5–10 years tripled. In the first half of the study period, there were no return periods of the highest surge level exceeding 10 years. However, in the second half, there were 3 records with return periods of more than 10 years, and one of them was more than 20 years. It can be concluded that the frequency of the storm surges increased in the second half of study period, especially the frequency of storm surges having the highest surge level with longer return periods.

As shown in Figure 12, the return periods of the adjusted direct economic losses were mainly located in the group with a 1–2 year return period. In the group with a return period of 1–2 years, the records for the second half increased dramatically from 31 times to 48 times. The frequency in the group with 2–5 years reduced from 3 to 2. The frequency in the group with 5–10 years remained stable at 1. During the first half of the research period, there were two records located in the group with 20–50 years among all return period groups whose return periods were longer than 10 years. In the second half, no storm surge events with return periods of adjusted direct economic loss greater than 10 years were recorded. No significant trends in the return periods of the adjusted direct economic loss were found after comparing the frequencies in the two halves in contrast with the increasing trend of the frequency of the return periods of the highest surge level, which indicates the changes in climate have less effect on the economy of the coastal region than does the hydrologic aspect. This may result from better storm-surge disaster mitigation in recent years.

DISCUSSION

The parameter estimation methods (the least-squares method, the Thomas plot method, and the moment method) performed well based on error-evaluation results, and most of the goodness-of-fit test results were very close. However, the performance of the least-squares method performed relatively better in the error-evaluation analysis of the distributions of both the highest surge levels and the adjusted direct economic losses. In this case, the least-squares method was determined to be the best method for parameter estimation, and the parameters derived from it were used in the final distribution functions. According to the observed data in Figures 4 and 6, the distribution functions fit the data well. However, there are some up-to-date methods for estimating extreme value distributions, and those parameters could be more precise than the methods used in this article (Skjong, Naess, and Naess, 2013); therefore, it may be worthwhile to evaluate them in further research.

In this study, the least-squares method was chosen to determine the final distributions for calculating both the highest surge level and the adjusted direct economic loss. However, previous research carried out by Hu *et al*. (1993) showed that the Thomas plot method had better accuracy in estimating the parameters compared with the least-squares method and the moment method. These findings indicate that it is necessary to confirm the performance of the parameter-estimation methods by evaluating the errors individually and that the ideal parameter-evaluation method for different research samples is not consistent.

As shown in Figure 7, the movement of the adjusted direct economic loss line was not synchronous when the return periods of the highest surge level increased. The return period of the direct economic losses tended to be longer than those of the highest surge levels when the return periods of the highest surge level were shorter than 1.29 years. Storm surge events with minor surge levels often cause unexpected economic loss. This indicates that the damages caused by a storm surge are not completely determined by the level of the surge (Core Writing Team, Pachauri, and Meyer, 2014); therefore, even if the potential surge level is not high, advanced preparation should not be neglected. In addition, the economic loss caused by a storm surge is related to other indicators besides the surge level, such as the state of the local economic development, the storm intensity, the forward speed, the size, the angle of approach to the coast, the central pressure of the storm, and the shape and characteristics of the coastal features, such as bays and estuaries (NOAA, 2016). Therefore, the return period of a storm-surge level is a different concept from the return period of the direct economic losses caused by that storm surge. The

severity of a storm-surge disaster simply identified by the return period of the surge level can, occasionally, be misleading.

In addition, there are some limitations in this article. The data collected was on a national scale, and the data on the highest surge levels were gauged at different tidal stations in different spatial locations because storm surges were the intended research subject and the impacts of those surges were not fixed within the range of specific stations. Because of that assumption, some of the surge levels from different stations may be incomparable, which could lead to a negative influence on the accuracy of the analyses. In addition, the sample size was another limitation. The data were recorded between 1989 and 2014, and there were 88 events. Although all the storm-surge events were the most severe ones in each year, the shortness of records influenced the method selection for a more accurate conclusion. Furthermore, the time duration was not sufficient to identify the distribution for longer return periods.

CONCLUSIONS

The Gumbel distribution employed in this article has been widely used in a number of research fields. In this study, the application of the Gumbel distribution to identify the return periods of the highest surge levels and the adjusted direct economic losses was noticeably effective. The parameter-estimation methods (the least-squares method, the Thomas plot method, and the moment method) performed well and were analyzed by error evaluation. The least-squares method was identified as the best method of parameter estimation for both the highest surge level and the adjusted direct economic loss, and the estimated parameters derived from that method were used in the final distribution functions. The expressions of the distribution functions and the return periods for the highest surge level and the adjusted direct economic loss were generated and can be applied to storm-surge prediction, coastal engineering design, and the estimation of the damage of a disaster caused by a storm surge.

The relationships between the return periods of the highest surge level and the adjusted direct economic loss were also analyzed. The linear functional relationship was not significant. Storm-surge events with minor surge levels often caused unexpected economic losses, which indicates that the damages caused by a storm surge are not completely determined by the level of the surge. Therefore, even if the potential surge level is not high, disaster management plans made ahead of time are still necessary. The geographic analyses indicate that there are strong spatial autocorrelations between the highest surge levels and the adjusted direct economic losses. Both the highest surge level and the adjusted direct economic loss in CR1 tended to be smaller at the same return-period level, which indicates storm surges in CR1 were less frequent and have less intensity than do storm surges in the other regions. Analysis based on climate change shows that the frequency of the storm surges increased in the second half of study period, especially the frequency of storm surges having the highest surge level with longer return periods. This may be the evidence for the trend in the impacts of storm surges resulting from climate change.

ACKNOWLEDGMENTS

Support for this research was provided by the National Natural Science Foundation of China through Grants 41072176 and 41371496 and by the National Science and Technology Support Program of China through Grant 2013BAK05B04. This work was also supported by a National Research Foundation of Korea (NRF) grant funded by the Korea government (MSIP) through GCRC-SOP (No. 2011-0030013). The authors would like to thank Dr. Xianqing Lv for his careful review and useful suggestions. The manuscript benefited from insightful discussions with Dr. Ling Zhang.

LITERATURE CITED

Bali, T.G., 2003. The generalized extreme value distribution. *Economics Letters*, 79(3), 423–427.

Castillo, E., 1988. *Extreme Value Theory in Engineering*. New York: Academic, 389p.

CCCC First Harbor Consultants Staff, 1998. *Code of Hydrology for Sea Harbor*. Beijing: Ministry of Transport, P.R.C., *JTJ213-98*, 10p (in Chinese).

Coles, S., 2001. *An Introduction to Statistical Modeling of Extreme Values*. London: Springer, 209p.

Core Writing Team; Pachauri, R.K., and Meyer, L.A., 2014. *IPCC, 2014: Climate Change 2014: Synthesis Report. Contribution of Working Groups I, II and III to the Fifth Assessment Report of the Intergovernmental Panel on Climate Change*. Geneva, Switzerland: IPCC, 36p.

Dong, S.; Tao, S.; Lei, S., and Soarses C.G., 2013. Parameter estimation of the maximum entropy distribution of significant wave height. *Journal of Coastal Research*, 29(3), 597–604.

Dong, S.; Yu, Y., and Xu, B., 2005. Return values calculation of storm surge elevation in Rizhao area. *Periodical of Ocean University of China,* 35(4), 655–660.

Fan, D., 2006. Variations in tropical-cyclone activity and storm-surge devastation since the 1950s in China. *Gulf Coast Association of Geological Societies Transactions,* 56, 185–192.

Feng, J. and Jiang W., 2015. Extreme water level analysis at three stations on the coast of the northwestern Pacific Ocean. *Ocean Dynamics,* 65(11), 1383–1397.

Gumbel, E.J., 1958. *Statistics of Extremes*. New York: Columbia University Press, 32p.

Horn, D.P., 2015. Chapter 6—Storm surge warning, mitigation, and adaptation. *In:* Ellis, J.T.; Sherman, D.J., and Shroder, J.F., Jr. (eds.), *Coastal and Marine Hazards Risks and Disasters*. Amsterdam, The Netherlands: Elsevier, pp. 153–180.

Hsu, P.L. and Robbins, H., 1985. Complete convergence and the law of large numbers. *In:* Lai, T.L. and Siegmund, D. (eds.), *Herbert Robbins Selected Papers*. New York: Springer, pp. 337–348.

Hu, J.; Jiang, H.; Zhou, Q., and Lin, Z., 1993. The methods of computing climate extremes using Gumbel extremal distribution. *Journal of Ocean University of Qingdao,* 23(1), 43–51 (in Chinese).

Jenkinson, A.F., 1955. The frequency distribution of the annual maximum (or minimum) values of meteorological elements. *Quarterly Journal of the Royal Meteorology Society,* 81(348), 158–171.

Kim, Y.C.; Choi, M., and Cho, Y.S., 2012. Tsunami hazard area predicted by probability distribution tendency. *Journal of Coastal Research,* 28(5), 1020–1031.

Liu, D. and Ma, F., 1976. Probability distribution theory of extreme values applied in the multiyear wave height distribution calculation. *Acta Mathematicae Applicatae Sinica,* 1976(1), 23–37 (in Chinese).

Liu, X.; Shannon, J.; Voun, H.; Truijens, M.; Chi, H.L., and Wang, X., 2014. Spatial and temporal analysis on the distribution of active radio-frequency identification (RFID) tracking accuracy with the Kriging method. *Sensors,* 14(11), 20451–20467.

Mahdi, S. and Ashkar, F., 2004. Exploring generalized probability weighted moments, generalized moments and maximum likelihood

estimating methods in two-parameter Weibull model. *Journal of Hydrology,* 285(1–4), 62–75.
Nicholls, R.J. and Cazenave, A., 2010. Sea-level rise and its impact on coastal zones. *Science,* 328(5985), 1517–1520.
Nnaji, G.A.; Huang, W.; Gitau, M.W., and Clayton Clark, I.I., 2014. Frequency analysis of minimum ecological flow and gage height in Suwannee river, Florida. *In:* Huang, W. and Hagen, S.C. (eds.), *Climate Change Impacts on Surface Water Systems*. *Journal of Coastal Research,* Special Issue No. 68, pp. 152–159.
NOAA. *Storm Surge Overview*. http://www.nhc.noaa.gov/surge/.
Obeysekera, J. and Park, J., 2013. Scenario-based projection of extreme sea levels. *Journal of Coastal Research,* 29(1), 1–7.
Oliver, M.A., and Webster, R., 1990. Kriging: A method of interpolation for geographical information systems. *International Journal of Geographical Information System,* 4(3), 313–332.
Öztürk, S.; Bayrak, Y.; Çınar, H.; Koravos, G.C., and Tsapanos, T.M., 2008. A quantitative appraisal of earthquake hazard parameters computed from Gumbel I method for different regions in and around turkey. *Natural Hazards,* 47(3), 471–495.
Pickands, III, J., 1975. Statistical inference using extreme order statistics. *Annals of Statistics,* 3(1), 119–131.
Scotto, M.G. and Tobias, A., 1999. Parameter estimation for the Gumbel distribution. *Stata Technical Bulletin,* 8(43), 1–44.
Shi, X.; Liu, S.; Yang, S.; Liu, Q.; Tan, J., and Guo, Z., 2015. Spatial-temporal distribution of storm surge damage in the coastal areas of China. *Natural Hazards,* 79(1), 237–247.
Skjong, M.; Naess, A., and Naess, O.E.B., 2013. Statistics of extreme sea levels for locations along the Norwegian Coast. *Journal of Coastal Research,* 29(5), 1029–1048.
State Oceanic Administration, P.R.C., 2015. *China Oceanic Disasters Communiqué*. http://www.coi.gov.cn/gongbao/zaihai/.
Tobler, W.R., 1970. A computer movie simulating urban growth in the Detroit region. *Economic Geography,* 46(1), S234–S240.
Tsai, C.H.; Tzang, S.Y.; Hsiao, S.S.; Cheng, C.C., and Li, H.W., 2006. Coastal structure failures and coastal waves on the north coast of Taiwan due to typhoon Herb. *Journal of Coastal Research,* 22(2), 393–405.
Wang, L.; Sun, X.; Lu, K., and Xu D., 2012. A maximum-entropy compound distribution model for extreme wave heights of typhoon-affected sea areas. *China Ocean Engineering,* 26(1), 49–58.
Wang, X. and Chen, X., 1984. Calculation of return period for storm surges at several stations along the coast of China. *Marine Forecasts Service,* 1(1), 18–25 (in Chinese).
Yue, S.; Ouarda, T.B.M.J.; Bobee, B.; Legendre, P., and Bruneau, P., 1999. The Gumbel mixed model for flood frequency analysis. *Journal of Hydrology,* 226(1–2), 88–100.
Zhou, Z.; Liu, S.; Hua, H.; Chen, C.; Zhong, G., and Liu, H., 2014. Frequency analysis for predicting extreme precipitation in Changxing Station of Taihu Basin, China. *In:* Huang, H. and Hagen, S.C. (eds.), *Climate Change Impacts on Surface Water Systems*. *Journal of Coastal Research,* Special Issue No. 68, pp. 144–151.